THE EFFECT OF A SERRATED TRAILING EDGE ON SELF-NOISE REDUCTION OF A FLAT PLATE

Mahmoud Karimi, Paul Croaker, Con Doolan and Nicole Kessissoglou

School of Mechanical and Manufacturing Engineering
UNSW Australia, Sydney, NSW 2052, Australia
Email: m.karimi@unsw.edu.au

Abstract

The noise generated by a flat plate with both sharp and serrated trailing edges under quadrupole excitation is predicted using a periodic boundary element technique. The flat plate is modelled as a continuous structure with a finite repetition of small spanwise segments. As such, the matrix equation formulated by the periodic boundary element method for this acoustic scattering problem can be represented as a block Toeplitz matrix. To solve the linear system of equations, the original matrix is embedded into a larger and more structured matrix called the block circulant matrix. The discrete Fourier transform is then employed in an iterative algorithm to solve the block Toeplitz system. Noise reduction plots are shown as a function of source location at different frequencies illustrating the effects of serrated edges on the scattered acoustic field.

1. Introduction

Scattering of acoustic pressure fluctuations induced by boundary layer turbulent structures over the trailing edge geometry produces trailing edge noise. One of the first systematic studies of trailing edge noise was reported by Ffowcs Williams and Hall [1] based on the classical Lighthill's acoustic analogy [2]. They considered a turbulent eddy convecting past a sharp trailing edge and used the analytical Green's function of a semi-infinite plate to account for the scattering from the trailing edge geometry. Howe [3] and Roger and Moreau [4, 5] developed analytical Green's functions which include the effect of the finite chord length and finite thickness of the airfoil. These models take into account the back scattering of the sound by the leading edge. However, lifting surfaces with thick profiles or spanwise variations in geometry such as trailing edge serrations are not well represented by such analytical Green's functions based on vanishingly thin planes. Oberai et al. [6] calculated the far-field acoustic pressure generated by a model quadrupole source placed near the trailing edge of an airfoil. They showed that the scattered component of the far-field acoustic pressure is much greater than the incident component. Moreau and Doolan [7] conducted an experimental investigation on the effects of trailing edge serrations on a flat plate at low-to-moderate Reynolds number. It was found that trailing edge serrations can minimise broadband noise levels at low frequencies and a substantial attenuation of blunt vortex-shedding noise can be achieved at high frequencies without modifying the directivity of the radiated noise. It was shown that the noise reduction using serrated trailing edge depends on Strouhal number and serration wavelength. This work has shown that serrated edges do not reduce noise as expected by theory and in some cases, an increase in noise occurs. While there is some evidence that this is due to a rearrangement of the turbulent flow structures about the serrations [7], there are still unresolved details that require further investigation as serrations are clearly important to the silent flight properties and must be part of future noise reduction technologies.

Airfoils and hydrofoils are continuous structures that can be modelled using the periodic BEM technique by taking a strip of the structure in the spanwise direction. In this work, a periodic BEM technique is used to investigate noise reduction mechanism of a flat plate with serrated trailing edge under quadrupole excitation. Turbulent flow over an airfoil produces very complex noise sources. To assess the performance of serrated trailing edge in noise reduction, a quadrupole is adopted which represents a flow-noise source. The periodic acoustic problem is formulated as a block Toeplitz system. By exploiting the Toeplitz structure, the computational time and storage requirements to construct and solve the linear system are significantly reduced. To solve the linear system of equations, the original matrix is embedded into a larger and more structured matrix called the block circulant matrix. Discrete Fourier transform is then employed in an iterative algorithm to solve the block Toeplitz system. The performance of the serrated trailing edge in noise reduction is demonstrated by changing the source location along three different paths. The results are provided at four data recovery points and different frequencies.

2. Boundary element Formulation

Assuming a time harmonic dependence of the form $e^{-\mathrm{i}\omega t}$, the Helmholtz equation is given by

$$\Delta p(\mathbf{x}) + k_f^2 p(\mathbf{x}) = -F \tag{1}$$

where $p(\mathbf{x})$ is the acoustic pressure at field point $\mathbf{x}$, F is the source, Δ is the Laplacian operator, $k_f = \omega/c_f$ is the acoustic wave number, ω is the angular frequency and c_f is the speed of sound. Equation (1) can be written in a weak formulation after integrating by parts twice as follows [8]

$$c(\mathbf{x})p(\mathbf{x}) + \int_\Gamma \frac{\partial G(\mathbf{x},\mathbf{y})}{\partial n(\mathbf{y})} p(\mathbf{y})\,\mathrm{d}\Gamma(\mathbf{y}) = \mathrm{i}\omega\rho_f \int_\Gamma G(\mathbf{x},\mathbf{y}) v_f(\mathbf{y})\,\mathrm{d}\Gamma(\mathbf{y}) + p_{\text{inc}}(\mathbf{x}) \tag{2}$$

where ρ_f is the fluid density and $\mathrm{i} = \sqrt{-1}$ is the imaginary unit. The vector $\mathbf{n}(\mathbf{y})$ represents the outward normal vector at the point $\mathbf{y}$, $\partial/\partial n(\mathbf{y})$ is the normal derivative, $v_f(\mathbf{y})$ is the fluid particle velocity and $\mathbf{y}$ is a source point position on the boundary Γ. Solution of the Helmholtz equation can be obtained by calculating the incident acoustic pressure radiated by the source and applying it as a load to the boundary integral equation (2). $p_{\text{inc}}(\mathbf{x})$ is the acoustic pressure incident as a result of the acoustic source. $c(\mathbf{x})$ is a free-term coefficient and equals 1 in the domain interior and 0.5 on a smooth boundary. $G(\mathbf{x},\mathbf{y})$ is the free-space Green's function for the Helmholtz equation given by

$$G(\mathbf{x},\mathbf{y}) = \frac{e^{\mathrm{i}k_f r}}{4\pi r} \qquad \text{where} \qquad r = |\mathbf{x}-\mathbf{y}| \tag{3}$$

The sharp-edged strut examined in this work is considered as a rigid structure. Hence the fluid particle velocity at the strut surface is zero, that is, $v_f(\mathbf{y}) = 0,\ \mathbf{y} \in \Gamma$. The BEM formulation then becomes a linear system of equations which can be expressed as follows

$$\mathbf{T}\,\mathbf{a} = \mathbf{b} \tag{4}$$

where $\mathbf{T}$ is the coefficient matrix and $\mathbf{a}$, $\mathbf{b}$ represent the sound pressure and incident pressure at nodal points, respectively. For an acoustic scattering problem which includes periodic structures, the matrix equation formulated by BEM is a block Toeplitz matrix. An $mn \times mn$ matrix $\mathbf{T}$ is called a block Toeplitz matrix (BTM) if it has constant blocks along each diagonal. Hence, a BTM has the form:

$$\mathbf{T} = \begin{pmatrix} \mathbf{T}_0 & \mathbf{T}_{-1} & \cdots & \cdots & \mathbf{T}_{1-m} \\ \mathbf{T}_1 & \mathbf{T}_0 & \mathbf{T}_{-1} & \cdots & \mathbf{T}_{2-m} \\ \vdots & \mathbf{T}_1 & \ddots & \ddots & \vdots \\ \vdots & \vdots & \ddots & \ddots & \mathbf{T}_{-1} \\ \mathbf{T}_{m-1} & \mathbf{T}_{m-2} & \cdots & \mathbf{T}_1 & \mathbf{T}_0 \end{pmatrix} \tag{5}$$

where each $\mathbf{T}_i$ is an $n \times n$ matrix. The number of unique blocks corresponds to the number of periodic sections found on the boundary surface. In the present work, the BTM is not necessarily a symmetric matrix.

Matrix $\mathbf{T}$ is specified by its first block row and its first block column. An $m \times m$ Toeplitz matrix can be embedded into a $2m \times 2m$ circulant matrix [9]. In the present work, a similar approach is used to embed the $mn \times mn$ BTM into a $2mn \times 2mn$ block circulant matrix $\mathbf{C}$ which can be represented by rightward circular shifts of its first block row: $\mathbf{R} = \{\mathbf{T}_0 \quad \mathbf{T}_{-1} \quad \ldots \quad \mathbf{T}_{1-m} \quad \mathbf{0} \quad \mathbf{T}_{m-1} \quad \ldots \quad \mathbf{T}_1\}$. Note that an $n \times n$ zero matrix is also incorporated into matrix $\mathbf{R}$. Using this embedding, equation (4) can be written in the following form

$$\mathbf{C}\,\mathbf{a}' = \mathbf{b}' \qquad \Leftrightarrow \qquad \begin{bmatrix} \mathbf{T} & \mathbf{S} \\ \mathbf{S} & \mathbf{T} \end{bmatrix} \begin{bmatrix} \mathbf{a} \\ \mathbf{0} \end{bmatrix} = \begin{bmatrix} \mathbf{b} \\ \mathbf{z} \end{bmatrix} \tag{6}$$

The block circulant system in equation (6) is equivalent to a Toeplitz system expressed by equation (4). The difference between these two formulations is that the left-hand side vector $\mathbf{a}$ in equation (4) contains all the unknown quantities whereas in the block circulant system, there are unknown entries in both the left-hand and right-hand side vectors. That is, $\mathbf{a}'$ and $\mathbf{b}'$ are partially unknown since $\mathbf{a}$ and $\mathbf{z}$ are unknown. The proposed algorithm for solving Toeplitz equations by Ferreira and Domínguez [10] is extended to solve the block Toeplitz system. Only the first block row and column of the linear system must be computed and stored. Hence the storage of the linear system is significantly reduced. The computational time to construct the coefficient matrix is also considerably decreased.

3. Numerical Results

To investigate the noise reduction mechanism of a serrated trailing edge, a flat plate model was used which corresponds to the experiment conducted by Moreau et al. [7] in an anechoic wind tunnel. The flat plate used in both the experiment and the simulation has a span of 450 mm and a thickness of 6 mm. The leading edge of the main body is elliptical with a semi-major axis of 8 mm and a semi-minor axis of 3 mm, while the trailing edge is asymmetrically bevelled at an angle of 12°, as shown in Figure 1. This figure also illustrates the coordinate system used in this work, whereby z = 0 corresponds to the mid-span of the first segment. Two different trailing-edge plates are examined corresponding to a plate model with a straight, unserrated configuration and a plate model with serrations. In both models, the trailing edge thickness is 0.5 mm. The serrated trailing edge has a wavelength of $\lambda = 9$ mm with root-to-tip amplitude of $2h$ = 30 mm. The serrated model has a mean chord of 150 mm, so the area of the unserrated model equals the area of the serrated model.

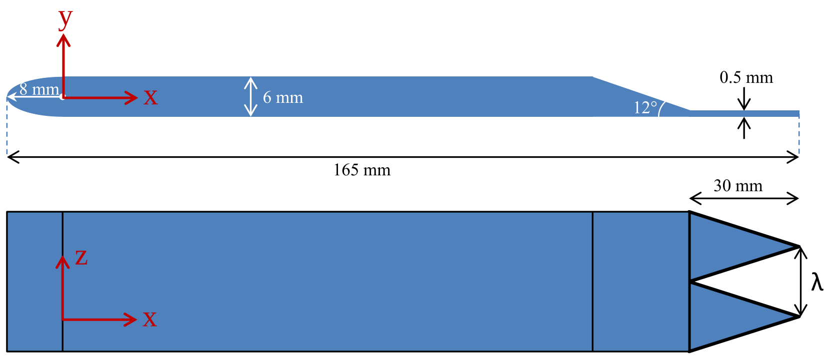

Figure 1 – Dimensions of the flat plate with serrated trailing edge

Two monopoles with opposite source-strengths separated by an infinitesimal distance $|\mathbf{d}|$ lead to a dipole. Analogously, two dipoles with opposite dipole moments $|\mathbf{d_m}|$ separated by an infinitesimal distance lead to a quadrupole. The incident pressure produced by the quadrupole is defined as the double spatial derivative of the harmonic free-field Green's function (equation (3)) and is given by [11]

$$p_{\text{inc}}(\mathbf{x}) = \mathrm{i}\omega\rho_f\,|\mathbf{d_m}|\,|\mathbf{d}|\,\frac{\partial^2 G\,(\mathbf{x},\mathbf{y})}{\partial y_1 \partial y_2} \tag{7}$$

Evaluation of the partial derivatives of the Green's function yields

$$p_{\text{inc}}(\mathbf{x}) = -\mathrm{i}\rho_f c_f k_f^3\,|\mathbf{d_m}|\,|\mathbf{d}|\,\frac{e^{\mathrm{i}k_f r}}{4\pi r}\left(\left(\frac{3}{k_f^2 r^2} - \frac{3\mathrm{i}}{k_f r} - 1\right)\frac{\partial r}{\partial y_1}\frac{\partial r}{\partial y_2}\right) \tag{8}$$

where $\mathbf{x}$ is the field point located at a collocation node and $\mathbf{y}$ is the location of the point quadrupole source. y_1 and y_2 are respectively the streamwise and vertical components of the acoustic source position vector. Sound attenuation by a serrated trailing edge is expressed in terms of noise reduction (NR) as follows

$$\mathrm{NR} = \mathrm{SPL}_{\text{unserrated trailing edge}} - \mathrm{SPL}_{\text{serrated trailing edge}} \tag{9}$$

where $\mathrm{SPL}_{\text{unserrated trailing edge}}$ and $\mathrm{SPL}_{\text{serrated trailing edge}}$ indicate the sound pressure levels at the same receiver positions with the unserrated and serrated trailing edges, respectively.

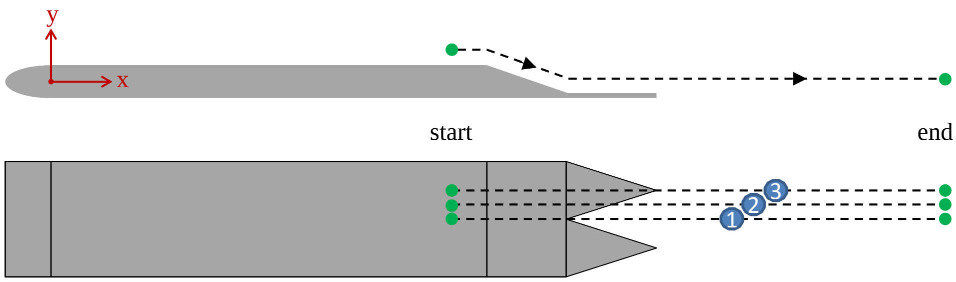

Figure 2 – Illustrative diagram of examined paths for the quadrupole source

The quadrupole is moved along three different paths placed 10 mm above the surface of the plate. These paths are shifted by a distance of $\lambda/4$ in the spanwise direction as shown in Figure 2. The start point of the paths is chosen just before where the inclined surface of the flat plate starts. The quadrupole is then moved in the positive x-direction with an increment of 2 mm towards the end point at x=200 mm. At each location the total far-field sound pressure level is computed at four different data recovery points, two above the plate named LE1 and TE1 and two below the plate called LE2 and TE2 located at a distance of 554 mm from the xz-plane. The results are provided for four different frequencies in Figures 3-6. The noise reduction is calculated based on the formula given by equation (9). It can be seen from the graphs that the results obtained from all three paths are almost identical except for the region above the inclined surface which they are distinguishable, particularly at low frequencies. The inclined surface starts at x=100 mm and is connected to the trailing edge at an x location of almost 128 mm. Generally, this analysis shows that implementation of serrations at trailing edge does not always lead to noise reduction and in some cases an increase in noise can occur. Basically, the performance of the serrations is dependent on the location of the noise source.

At 500 Hz, the noise reduction graphs show a similar trend for all four points. As the source moves above the inclined surface, the unserrated trailing edge produces less noise than the serrated edge. An upward trend in noise reduction can be observed when the source is moved along the trailing edge. Almost 33.5 dB noise reduction can be achieved when the source is located close to the tip of the trailing edge of the unserrated model. The performance of the serration is significantly decreased as the source moves downstream. As such, using the serration, the sound pressure level increases by almost 4 dB at all four data recovery points. It is apparent from the graphs that there is a sharp increase in noise reduction as the source is moved further away downstream and then the results level out at almost 2 dB. This investigation shows that maximum attenuation is achieved for all frequencies at all four data recovery points when the source point is located above the tip of the unserrated trailing edge, with the exception of TE1 at 3500 Hz and 5000 Hz where the maximum noise reductions occur when the source is at x=110 mm. The results also indicate that the absolute minimum in noise reduction graph for all the cases occur when the source is located where the bevelled surface joins the trailing edge except for TE1 at 2000 Hz and LE2 at 3500 Hz.

4. Conclusions

In this work, the noise reduction of a flat plate by implementing a serrated trailing edge under quadrupole excitation was investigated using a periodic boundary element technique. The matrix equation formulated by the periodic boundary element method for this acoustic scattering problem was a block Toeplitz matrix. To solve the linear system of equations, the original matrix was embedded into a larger and more structured matrix called the block circulant matrix. The discrete Fourier transform was then employed in an iterative algorithm to solve the block Toeplitz system. Noise reduction plots are shown as a function of source location at different frequencies. It was shown that maximum noise reduction can be achieved when the source is located near the tip of the trailing edge of the unserrated model.

5. Acknowledgement

The first author gratefully acknowledges the financial assistance provided by the Australian Acoustical Society NSW Division to attend the Acoustics 2015 conference.

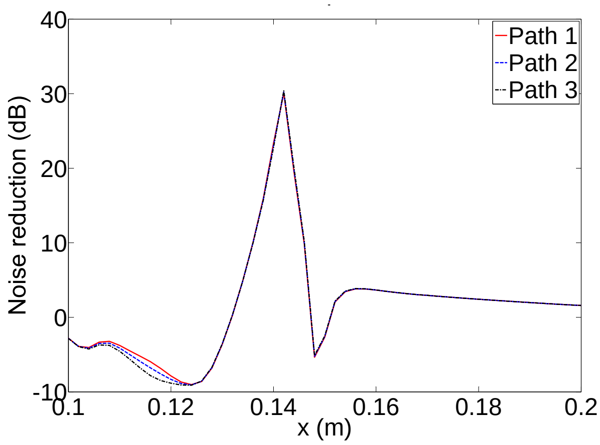

(a) LE1

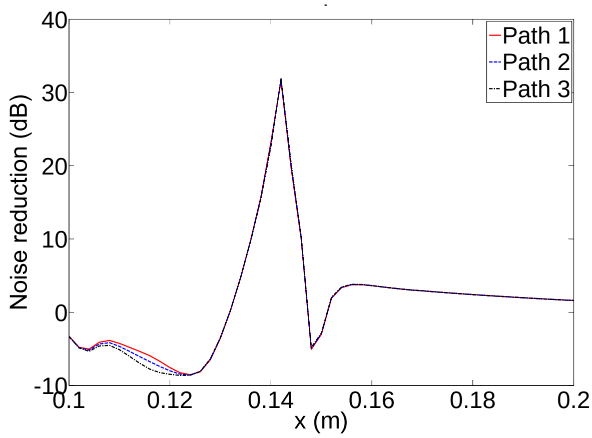

(b) LE2

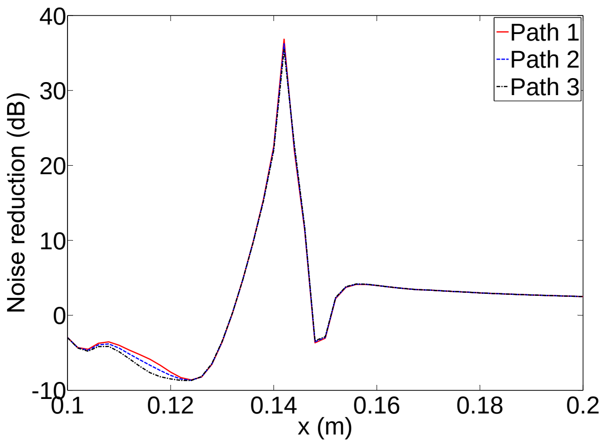

(c) TE1

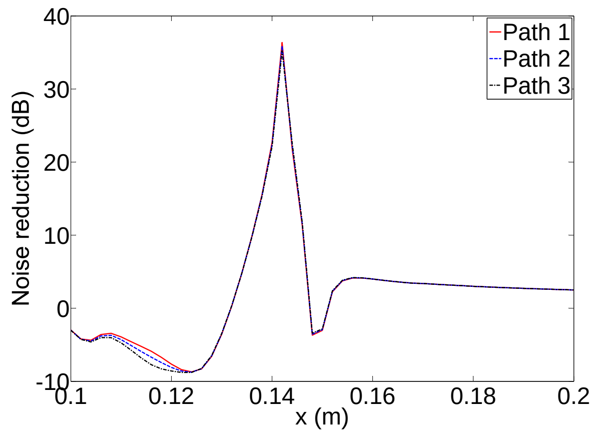

(d) TE2

Figure 3 – Noise reduction using serrated trailing edge as a function of quadrupole location along the x-direction for three different paths at 500 Hz

References

[1] Ffowcs Williams, J. E. and Hall, L. H., "Aerodynamic sound generation by turbulent flow in the vicinity of a scattering half plane", *Journal of Fluid Mechanics* 40(4) (1970), 657–670.

[2] Lighthill, M. J., "On sound generated aerodynamically", *Proceedings of the Royal Society Series A* 211 (1952), 564–587.

[3] Howe, M. S., "On the hydroacoustics of a trailing edge with a detached flap", *Journal of Sound and Vibration* 239(4) (2001), 801–817.

[4] Roger, M. and Moreau, S., "Broadband self-noise from loaded fan blades", *AIAA Journal* 42 (2004), 536–544.

[5] Roger, M. and Moreau, S., “Back-scattering correction and further extension of Amiet’s trailing-edge noise model. Part I: Theory”, *Journal of Sound and Vibration* 286 (2005), 477–506.

[6] Oberai, A., Roknaldin, F. and Hughes, T. J. R., “Computation of trailing edge noise due to turbulent flow over an airfoil”, *AIAA Journal* 40 (2002), 2206–2216.

[7] Moreau, D. J. and Doolan, C. J., “Noise-reduction mechanism of a flat-plate serrated trailing edge”, *AIAA Journal* 51(10) (2013), 2513–2522.

[8] Marburg, S. and Nolte, B., *Computational acoustics of noise propagation in fluids - Finite and boundary element methods,* Springer, 2008, 578.

[9] Golub, G.H. and Van Loan, C.F., *Matrix computations,* 2nd, Baltimore: Johns Hopkins University Press, 1989.

[10] Ferreira, P.J.S.G. and Domínguez, M. E., “Trading-off matrix size and matrix structure: Handling Toeplitz equations by embedding on a larger circulant set”, *Digital Signal Processing* 20(6) (2010), 1711 –1722.

[11] Pierce, A.D., *Acoustics: An introduction to its physical principles and applications,* Acoustical Society of America, 1991.

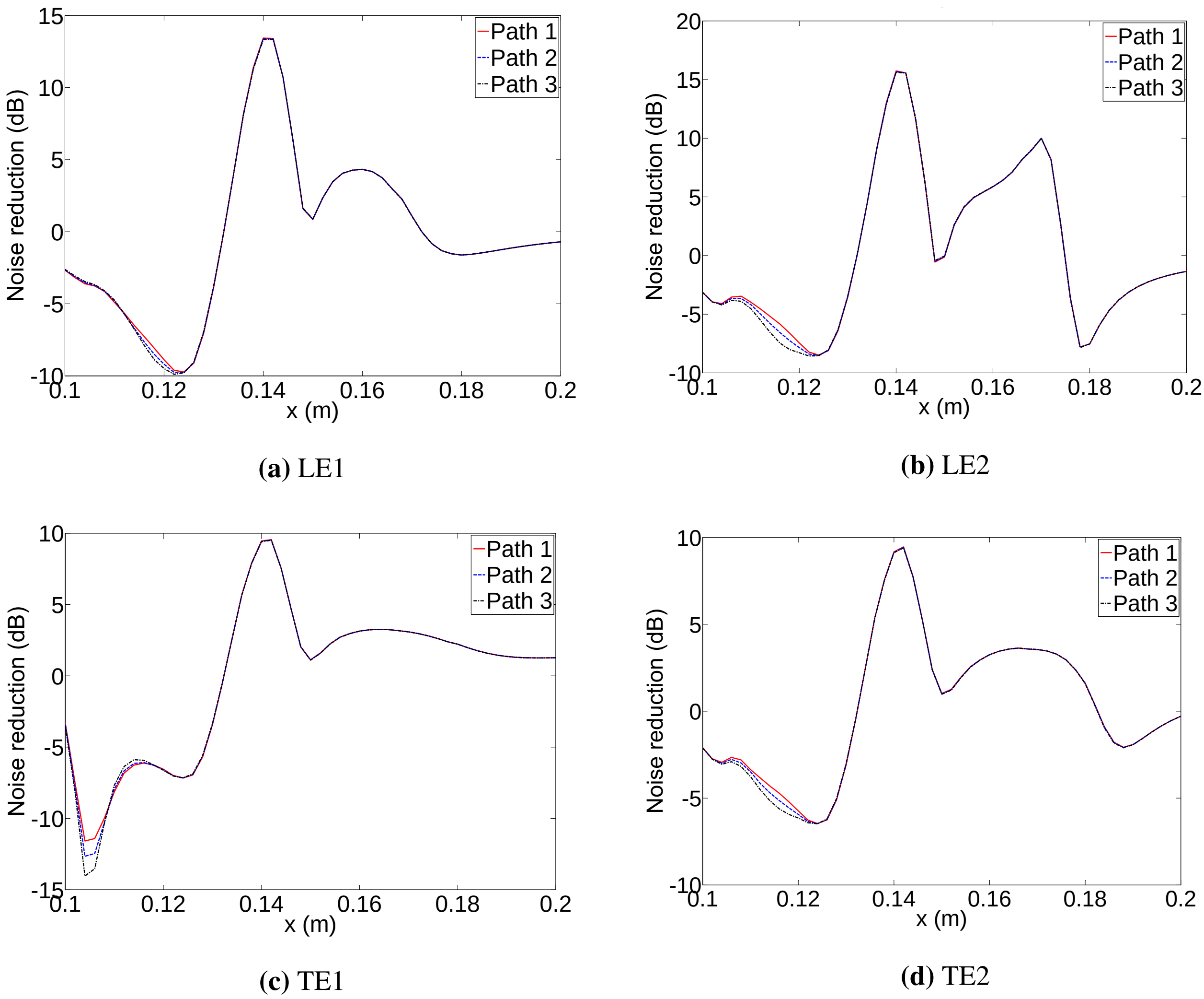

Figure 4 – Noise reduction using serrated trailing edge as a function of quadrupole location along the x-direction for three different paths at 2000 Hz

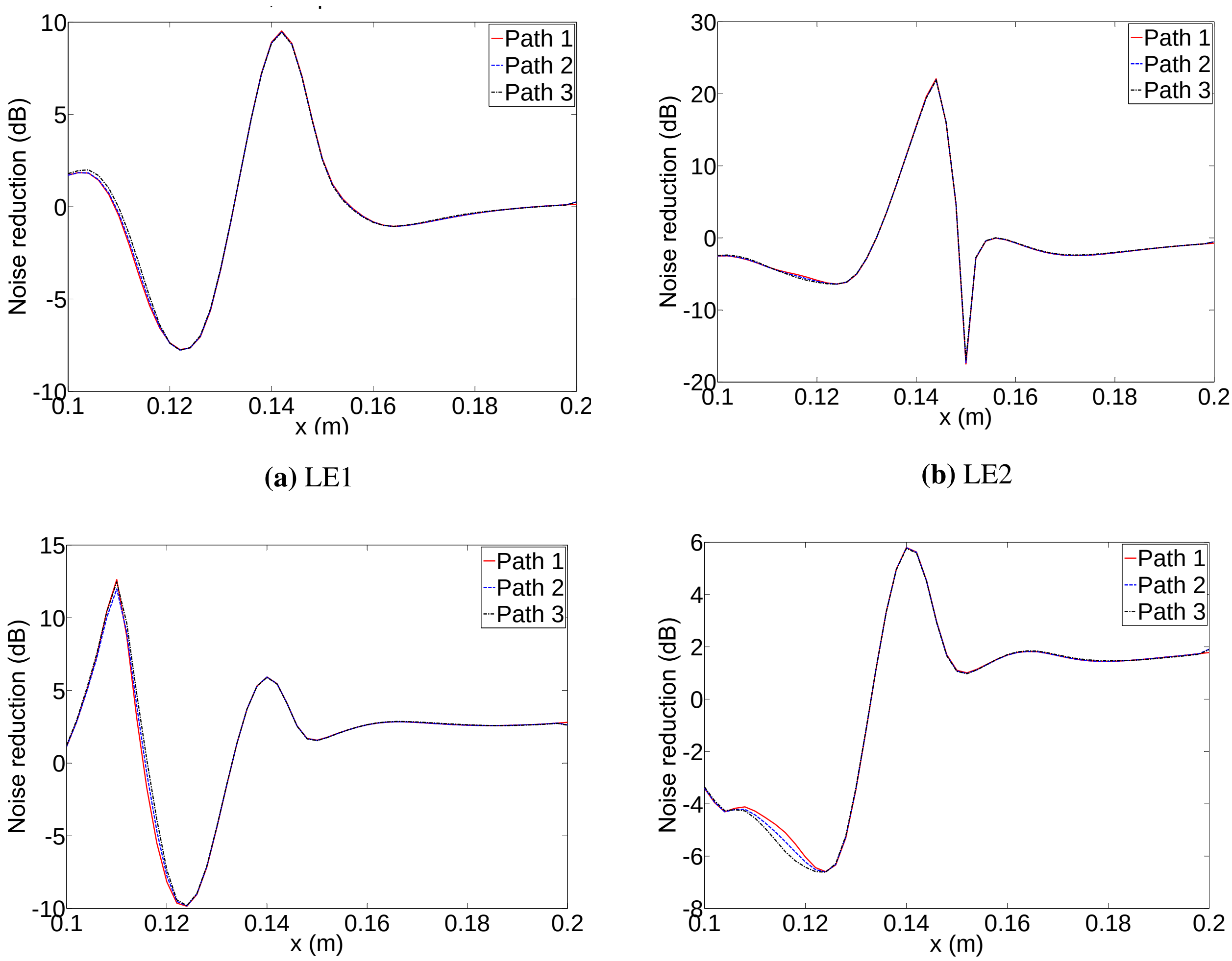

(a) LE1

(b) LE2

(c) TE1

(d) TE2

Figure 5 – Noise reduction using serrated trailing edge as a function of quadrupole location along the x-direction for three different paths at 3500 Hz

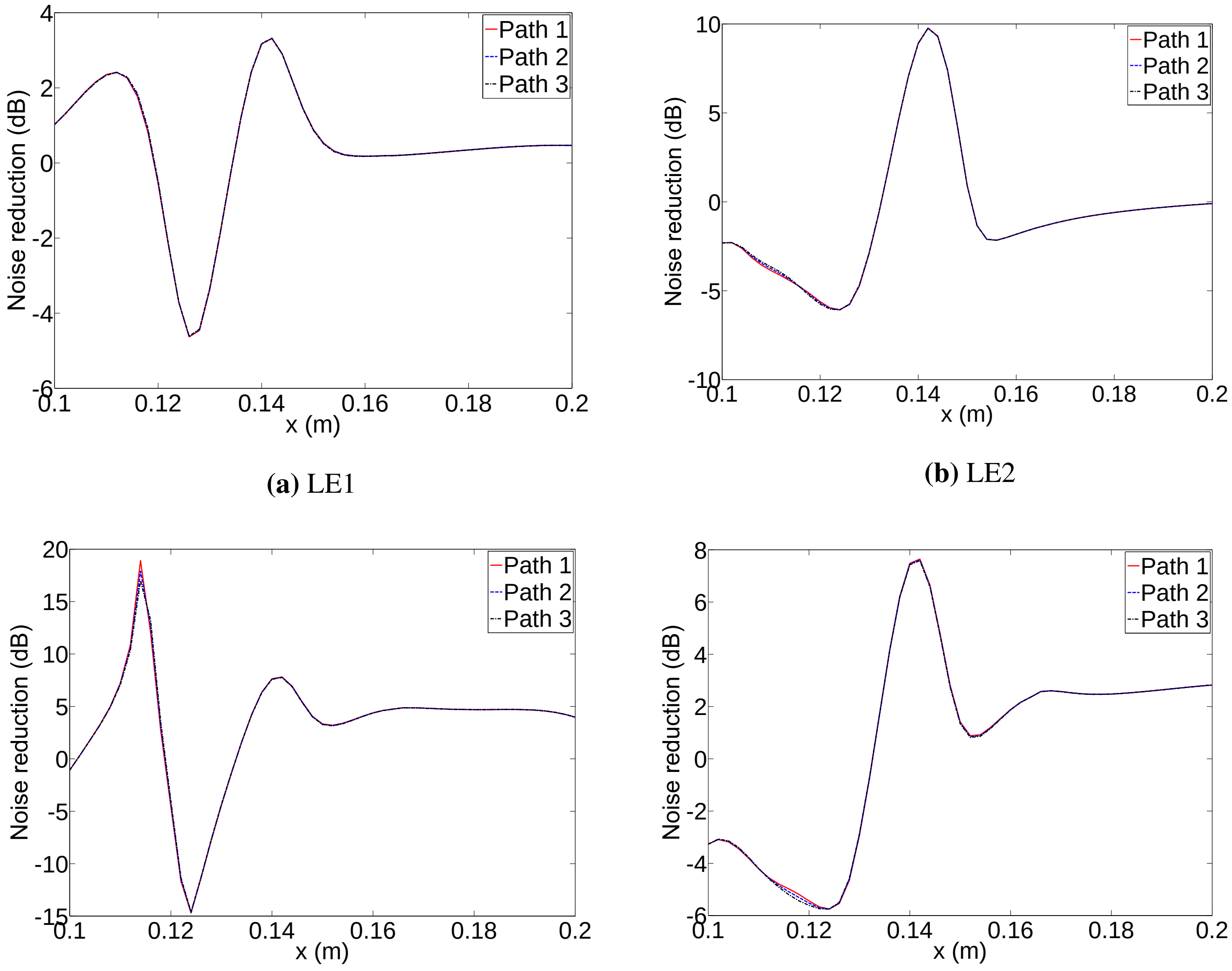

(a) LE1

(b) LE2

(c) TE1

(d) TE2

Figure 6 – Noise reduction using serrated trailing edge as a function of quadrupole location along the x-direction for three different paths at 5000 Hz